Suppression of finite-size effects in one-dimensional correlated systems

A. Gendiar[1,2,3], M. Daniška[1,4], Y. Lee[1,3], and T. Nishino[3]
[1] *Institute of Physics, Slovak Academy of Sciences, SK-845 11, Bratislava, Slovakia*
[2] *Institute of Electrical Engineering, Slovak Academy of Sciences, SK-841 04, Bratislava, Slovakia*
[3] *Department of Physics, Graduate School of Science, Kobe University, Kobe 657-8501, Japan*
[4] *Department of Nuclear Physics and Biophysics, Faculty of Mathematics, Physics and Informatics, Comenius University, SK-842 48 Bratislava, Slovakia*
(Dated: March 14, 2011)

We investigate the effect of a non-uniform deformation applied to one-dimensional (1D) quantum systems, where the local energy scale is proportional to $g_j = [\sin(j\pi/N)]^m$ determined by a positive integer m, site index $1 \le j \le N-1$, and the system size N. This deformation introduces a smooth boundary to systems with open boundary conditions. When $m \ge 2$, the leading $1/N$ correction to the ground state energy per bond $e_0^{(N)}$ vanishes and one is left with a $1/N^2$ correction, the same as with periodic boundary conditions. In particular, when $m = 2$, the value of $e_0^{(N)}$ obtained from the deformed open-boundary system coincides with the uniform system with periodic boundary conditions. We confirm the fact numerically for correlated systems, such as the extended Hubbard model, in addition to 1D free-Fermion models.

PACS numbers: 03.65.Aa, 05.30.Fk, 71.10.Fd

arXiv:1012.1472v2 [cond-mat.str-el] 11 Mar 2011

I. INTRODUCTION

The periodic boundary conditions (PBC) are often more convenient than the open boundary conditions (OBC), when asymptotic properties of one-dimensional (1D) quantum systems are studied in the thermodynamic limit. This is partially because boundary energy corrections exist under OBC, where eigenstates are not translational invariant. Systems with PBC normally contain smaller finite size effects, and this property of PBC is appropriate for accurate determination of bulk properties by means of the finite size scaling. [1–3]

In numerical studies of lattice models, OBC are often chosen for technical reasons. In particular, majority of the practical numerical analyses by the density matrix renormalization group (DMRG) method [4–6] are performed under OBC. Concerning to finite size systems with PBC, the crucial point in DMRG is the ring-shaped geometry, which reduces the decay rate of the singular values. [7] Although recent progress in DMRG and the tensor product formalisms made it possible to include the PBC in a natural manner, [7–10] numerical implementation requires additional computational resources compared with conventional DMRG analyses.

A way of suppressing the boundary energy corrections induced by OBC is to introduce smooth boundary conditions (SBC). [11, 12] Recently we proposed a variant of the smooth boundary conditions, where the local energy scale of N-site systems is proportional to the deformation function $[\sin(j\pi/N)]^2$ specified by the site index $1 \le j \le N-1$. [13, 14] This *sine-squared deformation* (SSD) [15] completely suppresses the boundary effects when the ground-state energy of a free-Fermions model on the 1D lattice is considered. In this article we generalize the deformation function, which is given by $g_j = [\sin(j\pi/N)]^m$, where m is a positive integer. [16] In the next section, we examine the effect of this *sinusoidal deformation* by g_j up to $m = 5$ when it is applied to the 1D free-Fermion model. It is shown that the case $m = 2$, the SSD, is the most efficient for the suppression of the boundary effect.

Another trial in this article is the application of SSD to correlated systems. As typical examples of correlated systems, we choose the spinless-Fermion model with nearest-neighbor interaction and the extended Hubbard model; we report the numerical result obtained by DMRG in Sec. III. When the interaction is present, the determination of the chemical potential is non trivial. We present a systematic way of solving this problem in Sec. IV. We summarize results in the last section.

II. SINUSOIDAL DEFORMATION

We start from the sinusoidal deformation applied to the free-Fermion model on the 1D lattice. Consider a tight-binding model represented by the Hamiltonian

$$\mathcal{H}^{(N)} = -t \sum_{j=1}^{N-1} \left(c_j^\dagger c_{j+1} + c_{j+1}^\dagger c_j \right) - \alpha\, t \left(c_N^\dagger c_1 + c_1^\dagger c_N \right), \tag{1}$$

where N is the system size, and t the hopping energy. Operators $c_j^\dagger$ and c_j represent creation and annihilation of Fermions, respectively. The parameter α specifies the boundary condition, where OBC and PBC correspond to $\alpha = 0$ and $\alpha = 1$, respectively. (The choice $\alpha = -1$ is known as the anti-periodic boundary conditions, which we do not treat in this article.) For each boundary condition, the one-particle energy is expressed as

$$\varepsilon_\ell = \begin{cases} -2t\cos\left(\dfrac{\pi\ell}{N+1}\right) & \text{for OBC } (\alpha=0)\,, \\ -2t\cos\left(\dfrac{2\pi\ell}{N}\right) & \text{for PBC } (\alpha=1)\,, \end{cases} \tag{2}$$

where the energy index ℓ runs from 1 to N. The ground-state energy $E_0^{(N)}$ at half filling is obtained as the sum of ε_ℓ below the Fermi energy $\varepsilon_{\rm F}=0$.

Throughout this article we focus on the system size dependence on the energy per site $E_0^{(N)}/N$ or the energy per bond, which is $E_0^{(N)}/N$ under PBC and is $E_0^{(N)}/(N-1)$ under OBC. After a short algebra, one obtains

$$\frac{E_0^{(N)}}{N} = -\frac{2t}{\pi} + \frac{t}{N}\left(1-\frac{2}{\pi}\right) + \mathcal{O}\left(\frac{1}{N^2}\right) \tag{3}$$

with OBC, where the leading order of the finite size correction is proportional to N^{-1}. The correction of the same order also exists for the energy per bond. With PBC, one finds

$$\frac{E_0^{(N)}}{N} = -\frac{2t}{\pi} + \frac{2\pi t}{3N^2} + \mathcal{O}\left(\frac{1}{N^3}\right)\,, \tag{4}$$

where the leading correction is of the order of N^{-2}. The difference between Eq. (3) and Eq. (4) chiefly comes from the presence of the boundary energy which exists only when OBC are imposed.

The sinusoidal deformation introduces a position dependent energy scale $g_j = \left[\sin(j\pi/N)\right]^m$ to each bond of the system with OBC, where m is the positive integer. [13, 14] Deforming $\mathcal{H}^{(N)}$ in Eq. (1), we obtain the corresponding free-Fermionic Hamiltonian

$$\mathcal{H}_{\rm sine}^{(N)} = -t\sum_{j=1}^{N-1}\left[\sin\left(\frac{j\pi}{N}\right)\right]^m\left(c_j^\dagger c_{j+1} + c_{j+1}^\dagger c_j\right)\,. \tag{5}$$

We have not obtained analytical solution for the one-particle spectrum of $\mathcal{H}_{\rm sine}^{(N)}$ so far, except for the zero-energy state. Thus we perform numerical analyses in the following investigations on the ground state.

Since we are interested in the ground-state energy per site (or per bond), we introduce the normalization factor

$$B^{(N)} = \sum_{j=1}^{N-1}\left[\sin\left(\frac{j\pi}{N}\right)\right]^m = \sum_{j=1}^{N-1} g_j\,, \tag{6}$$

which is the sum of the deformation factors over the entire system. When m is an odd positive integer, we have

$$B^{(N)} = \sum_{\ell=0}^{(m-1)/2}\frac{(-1)^\ell}{(2\ell)^{m-1}}\binom{m}{\ell}\cot\left[\frac{(m-2\ell)\pi}{2N}\right] \tag{7}$$

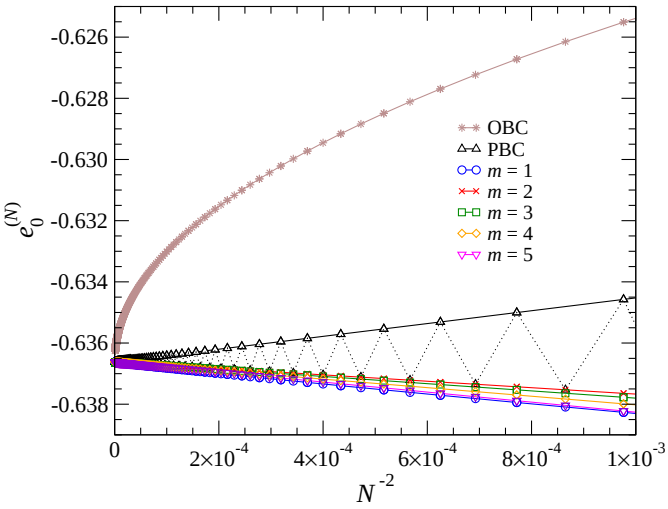


FIG. 1: (Color online) Convergence of $e_0^{(N)}$ in Eq. (9) with respect to N at half filling. Data with OBC, PBC, and the deformed cases with $m=1$ to 5 are shown.

and when m is an even positive integer, we have

$$B^{(N)} = \frac{N}{2^m}\binom{m}{m/2}\,. \tag{8}$$

We represent the ground-state energy of $\mathcal{H}_{\rm sine}^{(N)}$ at half filling by the notation $E_0^{(N)}$. It is expected that the normalized energy

$$e_0^{(N)} = \frac{E_0^{(N)}}{B^{(N)}} \tag{9}$$

converges to $-2t/\pi$ in the large N limit in analogy to Eqs. (3) and (4). We refer $e_0^{(N)}$ in Eq. (9) to as the energy per bond in the following. As a convention, we set $B^{(N)}=N-1$ for the system with OBC, and $B^{(N)}=N$ with PBC, where these values just represent the number of bonds. Using this extended definition of $B^{(N)}$, we can represent energy per bond by Eq. (9) regardless of the boundary condition or the presence of deformation.

We regard t as the unit of the energy in the numerical analyses. Figure 1 shows the N-dependence of $e_0^{(N)}$ in Eq. (9) for the undeformed systems with OBC, PBC, and the deformed systems from $m=1$ to 5. When the PBC are imposed, the convergence of $e_0^{(N)}$ with respect to N^{-2} is linear, and there is even-odd oscillation with respect to the particle number $N/2$. Similarly the linear N^{-2}-dependence is observed when $m\geq 2$ under the sinusoidal deformation. In the case $m=1$, there is additional logarithmic correction as shown later. It should be noted that when the particle number $N/2$ is odd, $e_0^{(N)}$ obtained with the sinusoidal deformation for $m=2$ coincides with $e_0^{(N)}$ obtained with PBC. [17] This complete agreement is checked down to the smallest digit in numerical precision. Throughout this paper we use the exact diagonalization in order to reduce any numerical errors to minimum.

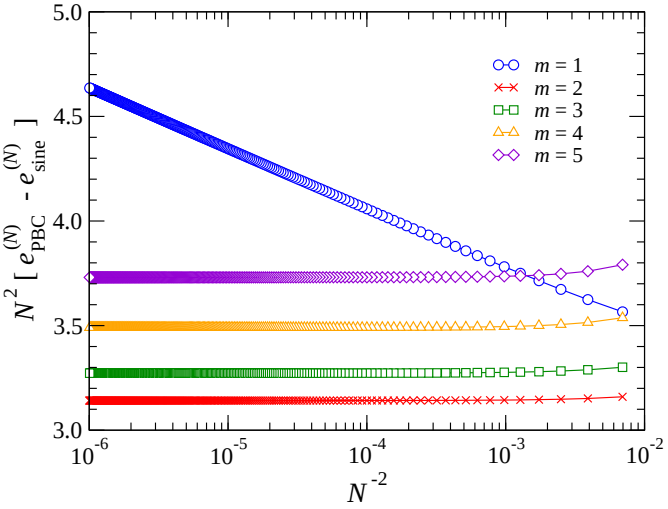


FIG. 2: (Color online) Asymptotic behavior of $e_0^{(N)}$ for the deformed chains when $1 \le m \le 5$ with respect to $e_0^{(N)}$ of the system with PBC. A logarithmic correction is present when $m = 1$.

In order to confirm the N^{-2}-dependence of $e_0^{(N)}$ with the sinusoidal deformation under $m \ge 2$, we plot the difference between $e_0^{(N)}$ obtained with PBC (when $N/2$ is even) and $e_0^{(N)}$ with the sinusoidal deformation. To avoid any confusion, let $E_{\rm PBC}^{(N)}$ and $E_{\rm sine}^{(N)}$ denote the ground-state energy obtained with PBC and with the sinusoidal deformation, respectively. We also use a similar notation for the normalization factors $B_{\rm PBC}^{(N)} = N$ and $B_{\rm sine}^{(N)}$ for the normalization factor defined in Eq. (6). Figure 2 depicts the magnified difference

$$N^2 \left[e_{\rm PBC}^{(N)} - e_{\rm sine}^{(N)} \right] \equiv N^2 \left[\frac{E_{\rm PBC}^{(N)}}{B_{\rm PBC}^{(N)}} - \frac{E_{\rm sine}^{(N)}}{B_{\rm sine}^{(N)}} \right] \qquad (10)$$

when N is even. It is shown that the logarithmic correction $(N \log N)^{-1}$ is present when $m = 1$, and is absent when $m \ge 2$.

Figure 3 shows the spatial distribution of the bond correlation function $\langle c_j^\dagger c_{j+1} + c_{j+1}^\dagger c_j \rangle$ at half filling when $N = 1000$. The Friedel oscillations induced by the boundary are clearly observed when OBC are imposed (the asterisks), and weaker oscillations are observed with the sinusoidal deformation when $m = 1$. Only when $m = 2$, there are no oscillations at all; we checked the uniformity (the translation invariance) of the bond correlation function down to the 16-digits in numerical precision. When $m \ge 3$, the boundary effects appear again. In this case the bond correlation function toward the system boundary does not oscillate, and decreases in monotonic manner. Such behaviors for each m might be related to the suppression of the boundary corrections in $e_0^{(N)}$.

We compare the efficiency of SSD ($m = 2$) with the SBC proposed in Ref. [11, 12]. Figure 4 shows the bond correlation function for both cases at half-filling, where

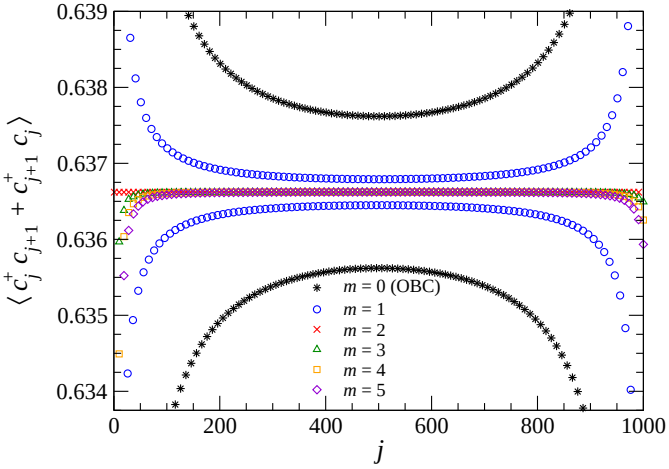


FIG. 3: (Color online) Expectation value of the bond correlation function $\langle c_j^\dagger c_{j+1} + c_{j+1}^\dagger c_j \rangle$ with respect to j under sinusoidal deformation.

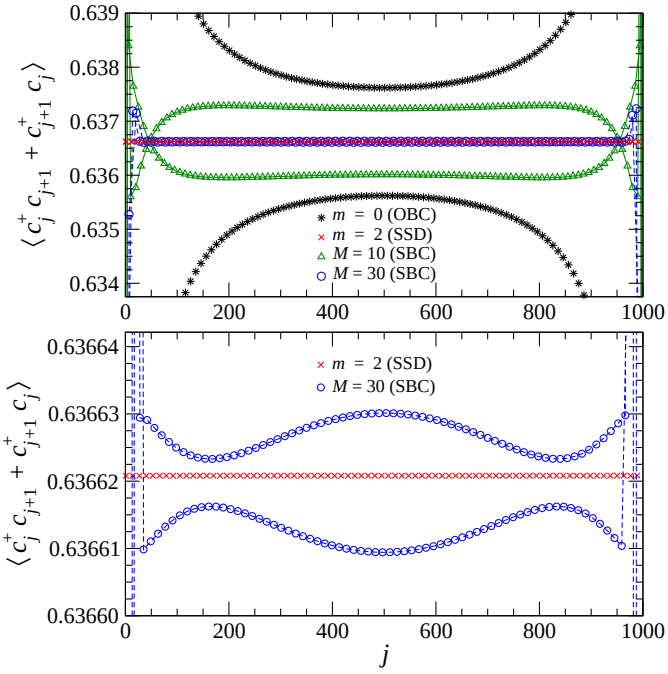


FIG. 4: (Color online) Comparison of the expectation value of the bond correlation function at half filling under SSD ($m = 2$) and SBC in Ref. [11, 12]. The number M in the case of SBC specifies the length of area where the interactions are modified near the system boundary. The bottom graph shows the numerical details when $M = 30$ (SBC) with respect to SSD.

the length of boundary area in SBC is chosen as $M = 10$ and $M = 30$ when the system size is $N = 1000$. Although bulk property is well captured by SBC already for $M = 30$, boundary fluctuations are still present. On the other hand, the bond correlation function is almost uniform away of the boundary.

Now we discuss the way of treating the deformed sys-

tem away from half filling. For the undeformed systems with OBC or PBC, it is sufficient to include the chemical potential term $-\mu \sum_{j=1}^{N} n_j$ into Eq. (1), where $n_j = c_j^\dagger c_j$ is the number operator. The value of μ adjusts the Fermi energy to zero, and is given by

$$\mu(f) = -2t \cos(\pi f)\,, \tag{11}$$

where f is the filling factor

$$f = \frac{1}{N} \sum_{j=1}^{N} \langle n_j \rangle\,. \tag{12}$$

A natural way of introducing $\mu(f)$ under the sinusoidal deformation is to write down the Hamiltonian as a sum of the local terms

$$\mathcal{H}_{\rm sine}^{(N)} = \sum_{j=1}^{N-1} \left[\sin\left(\frac{j\pi}{N}\right)\right]^m h_{j,j+1} = \sum_{j=1}^{N-1} g_j\, h_{j,j+1}\ , \tag{13}$$

where $\mu(f)$ is included to the bond operator

$$h_{j,j+1} = -t\left(c_j^\dagger c_{j+1} + c_{j+1}^\dagger c_j\right) - \frac{\mu}{2}\left(n_j + n_{j+1}\right)\ . \tag{14}$$

In order to confirm the validity of these constructions in Eqs. (11)-(14), we carried out numerical calculations for the selected fillings $f = 1/4$ and $f = 1/8$. Figure 5 shows the N^{-2}-dependence of $e_0^{(N)} = E_0^{(N)}/B^{(N)}$, where $E_0^{(N)}$ is the ground-state energy for each filling. We plot the data only when the particle number $p \equiv fN$ is even. Analogous to half filling, the bond energy $e_0^{(N)}$ with PBC coincides with that obtained with SSD ($m = 2$) when p is odd. [17] The logarithmic corrections are again present when $m = 1$.

The uniformity of the ground state obtained with the sinusoidal deformation is checked by calculating the occupancy $\langle n_j \rangle = \langle c_j^\dagger c_j \rangle$ at $f = 1/2$, $1/4$, and $1/8$. Figure 6 shows $\langle n_j \rangle$ when $m = 1$, 2, and 3. At half filling, $f = 1/2$, $\langle n_j \rangle$ is always equal to $1/2$ by the particle-hole symmetry. Even away from the half filling, this uniformity is kept when $m = 2$. There are small fluctuations near the system boundary when $m = 1$ and $m = 3$. In this way, the construction of Hamiltonian in Eqs. (13) and (14) away from half-filling is justified, especially for SSD.

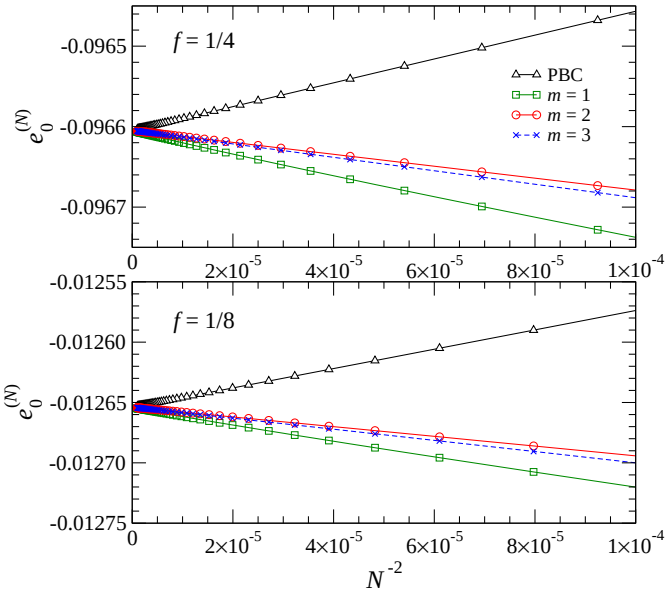


FIG. 5: (Color online) Convergence of $e_0^{(N)}$ with respect to N^{-2} at 1/4-filling and 1/8-filling.

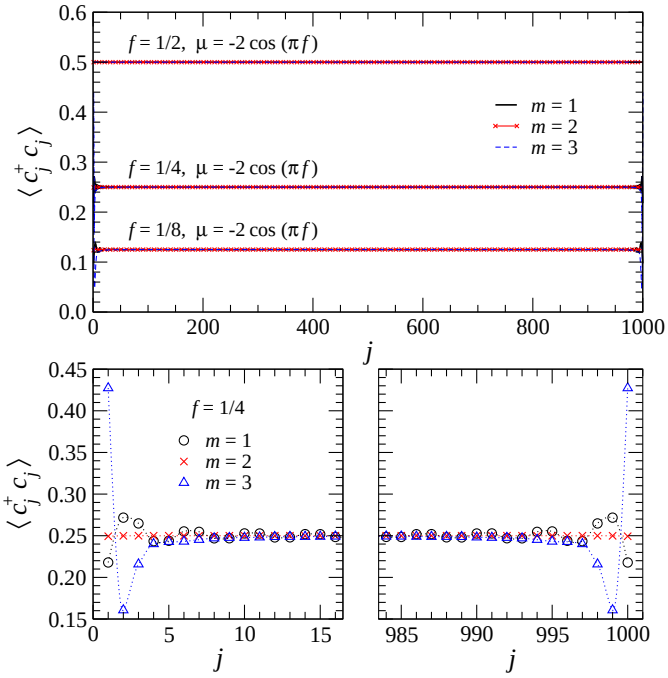


FIG. 6: (Color online) Position dependence of the occupation number $\langle n_j \rangle = \langle c_j^\dagger c_j \rangle$ at $f = 1/2$, $1/4$, and $1/8$ when $m = 1$, 2, and 3 (upper graph). The left and the right lower graphs display the occupancy at $f = 1/4$ close to the boundaries.

III. CORRELATED SYSTEMS

It is expected that the SSD reduces boundary effect even when interactions are present between particles. In order to check this conjecture, we apply the sinusoidal deformation to correlated systems, by means of the Hamiltonian Eq. (13) written in the linear combination of bond operators. We study the system size dependence of the ground-state energy $E_0^{(N)}$ and the uniformity of the system.

A. Spinless Fermions

As an example, let us consider spinless Fermions on the 1D lattice, whose behavior is described by the uniform

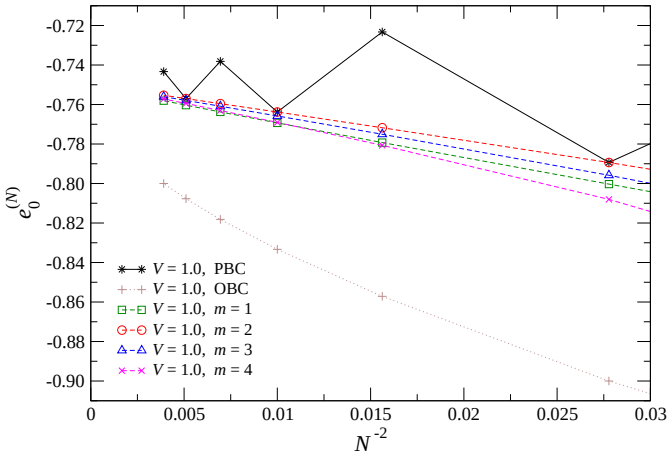


FIG. 7: (Color online) Energy per bond $e_0^{(N)}$ of the spinless Fermions model at $V = 1$ up to $N = 16$.

Hamiltonian

$$\mathcal{H}^{(N)}_{\rm PBC} = - t\sum_{j=1}^{N}\left(c_j^\dagger c_{j+1} + c_{j+1}^\dagger c_j\right) + V\sum_{j=1}^{N}\left(c_j^\dagger c_j - \frac{1}{2}\right)\left(c_{j+1}^\dagger c_{j+1} - \frac{1}{2}\right) \quad (15)$$

with PBC, where the system contains the repulsive Coulomb interaction $V > 0$ between neighboring sites, in addition to the hopping amplitude t. In this section we restrict ourselves to the half-filled case only, therefore the chemical potential μ is zero. [18] The construction of the Hamiltonian with OBC and its sinusoidal deformation is analogous to what we have done in the previous section. The deformed Hamiltonian can be defined by putting the bond operator as

$$h_{j,j+1} = - t\left(c_j^\dagger c_{j+1} + c_{j+1}^\dagger c_j\right) + V\left(c_j^\dagger c_j - \frac{1}{2}\right)\left(c_{j+1}^\dagger c_{j+1} - \frac{1}{2}\right) \quad (16)$$

and substituting it to Eq. (14). We calculate the ground state and the corresponding energy $E_0^{(N)}$ at half-filling up to $N = 16$.

Figure 7 shows $e_0^{(N)}$ with respect to N^{-2}. When the sinusoidal deformation is applied, we observe the same N^{-2} dependence as was seen for the non-interacting case. In particular when $N/2$ is odd, $e_0^{(N)}$ obtained for $m = 2$ shows a good agreement with the result from PBC. The coincidence, however, becomes less accurate with increasing V, and there is a deviation around 0.2% in $e_0^{(N)}$ when $V = 5$. Figure 8 shows the occupation number $\langle n_j\rangle$ and the bond correlation $\langle c_j^\dagger c_{j+1} + c_{j+1}^\dagger c_j\rangle$ when $V = 1$ at half filling. A clear uniformity is observed when $m = 2$ as shown in the non-interacting cases.

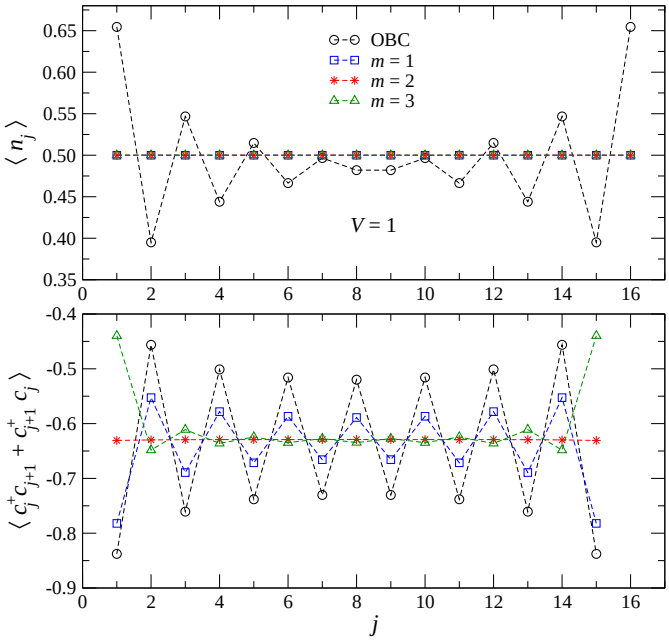


FIG. 8: (Color online) Occupation number $\langle n_j\rangle$ and the bond energy $\langle c_j^\dagger c_{j+1} + c_{j+1}^\dagger c_j\rangle$ when $V = 1$ at half filling.

B. Extended Hubbard Model

Now we consider the extended Hubbard model, which contains the on-site Coulomb interaction U and the neighboring interaction V. In this case there is spin degree of freedom ($\sigma = \uparrow, \downarrow$), therefore creation and annihilation operators, respectively, are represented as $c_{j\sigma}^\dagger$ and $c_{j\sigma}$. The bond operator of the extended Hubbard model is represented as

$$\begin{aligned} h_{j,j+1} = & - t\sum_{\sigma=\uparrow,\downarrow}\left(c_{j\sigma}^\dagger c_{j+1\sigma} + c_{j+1\sigma}^\dagger c_{j\sigma}\right) \\ & + \frac{U}{2}\Big[\left(n_{j\uparrow} - \tfrac{1}{2}\right)\left(n_{j\downarrow} - \tfrac{1}{2}\right) \\ & \quad + \left(n_{j+1\uparrow} - \tfrac{1}{2}\right)\left(n_{j+1\downarrow} - \tfrac{1}{2}\right)\Big] \\ & + V\left(n_{j\uparrow} + n_{j\downarrow} - 1\right)\left(n_{j+1\uparrow} + n_{j+1\downarrow} - 1\right). \end{aligned} \quad (17)$$

To avoid the complexity of determining the chemical potential μ, we consider the half-filled case where $\mu = 0$ is guaranteed by the particle hole symmetry. Figure 9 shows the N^{-2}-dependence of $e_0^{(N)}$ for various combinations of U and V. The coincidence between PBC and SSD at half filling occurs when the total number of both up- and downs-spin Fermions are odd.

The occupancy $\langle n_j\rangle = \langle n_{j\uparrow} + n_{j\downarrow}\rangle$ and the bond correlation function $\sum_\sigma\langle c_{j\sigma}^\dagger c_{j+1\sigma} + c_{j\sigma}^\dagger c_{j+1\sigma}\rangle$ at half filling are shown in Fig. 10. The occupancy $\langle n_j\rangle$ with OBC is clearly influenced by the system boundaries, whereas the sinusoidal deformations ($m \geq 1$) lead to almost constant distribution. The case with $m = 2$ (asterisks) realizes

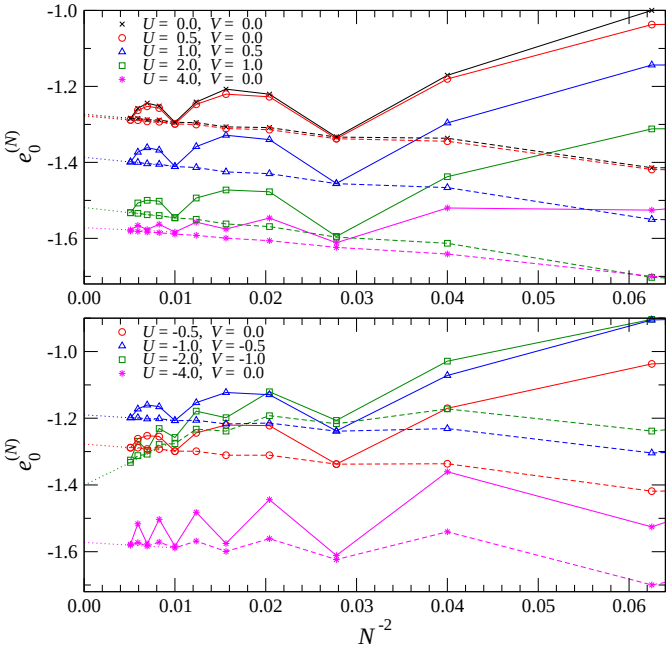


FIG. 9: (Color online) System size dependence of $e_0^{(N)}$ of the extended Hubbard model at half filling. The full and the dashed lines connect the energies $e_0^{(N)}$ obtained by PBC and SSD, respectively.

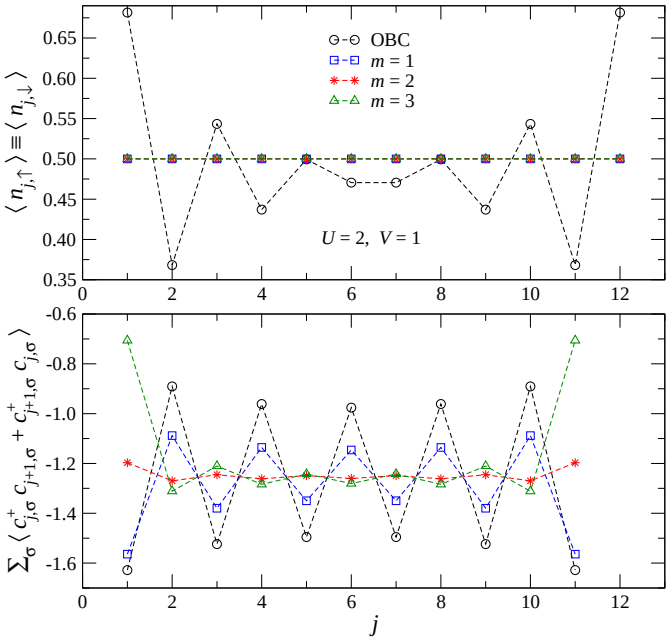


FIG. 10: (Color online) Occupation $\langle n_{j\uparrow}\rangle = \langle n_{j\downarrow}\rangle$ and the bond energy $\sum_\sigma \langle c^\dagger_{j\sigma}c_{j+1} + c^\dagger_{j+1\sigma}c_{j\sigma}\rangle$ of the extended Hubbard model at half filling.

the minimal position dependence. The bond correlation function is influenced by the boundaries in all cases, and the position dependence is the weakest when $m = 2$.

IV. CHEMICAL POTENTIAL

So far we have not discussed the proper value of the chemical potential μ away from the half filling when the interaction is present. The chemical potential term $-\frac{\mu}{2}(n_{j\uparrow} + n_{j\downarrow} + n_{j+1\uparrow} + n_{j+1\downarrow})$ has to be included to the bond operator in Eq. (18). In the Hartree-Fock or the Fermi liquid picture, μ is adjusted so that the particle number $p = \sum_{j=1}^{N}\langle n_{j\uparrow} + n_{j\downarrow}\rangle$ coincides with the number of negative-energy quasiparticle states. The number of particles is independently represented by the derivative of $E_0^{(N)}$ with respect to μ. Thus, the relation $p = -\partial E_0^{(N)}/\partial\mu$ must be satisfied for the targeted particle number p. Within the sinusoidal deformation, this relation is slightly modified as

$$p = -\frac{N}{B^{(N)}}\frac{\partial E_0^{(N)}}{\partial\mu} = -\frac{\partial N e_0^{(N)}}{\partial\mu} \qquad (18)$$

according to the position dependence in the energy scale.

We plot the absolute value $|p - (-\partial N e_0^{(N)}/\partial\mu)|$ with respect to μ for the extended Hubbard model in Fig. 11, under the SSD. The numerical analysis by exact diagonalization gives $\mu = -4.1425$ for the case $N = 12$, $p = 4$, $U = 2$, and $V = 1$. Figure 12 shows the corresponding

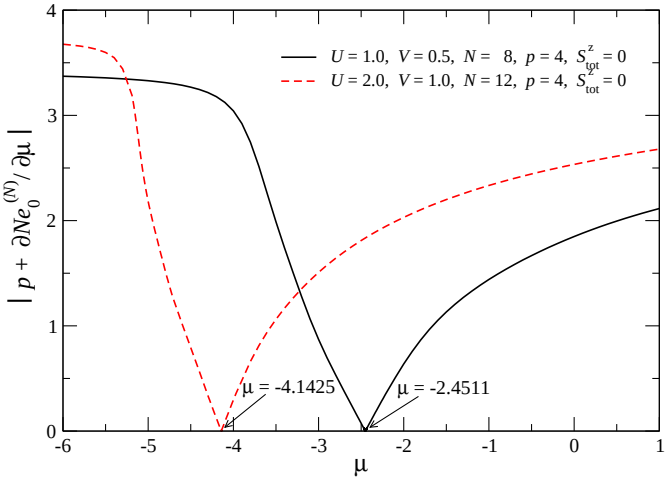


FIG. 11: (Color online) The μ dependence of $|p+\partial N e_0^{(N)}/\partial\mu|$ for the two cases $f \equiv p/2N = 1/4$ and $1/6$.

occupation and the bond correlation functions. There is a slight position dependence, since we are dealing with relatively small system size with a few particles. The position dependence becomes conspicuous if we choose either an inaccurate value of μ or we consider the deformations with $m \neq 2$.

V. CONCLUSION AND DISCUSSION

We have shown that the sinusoidal deformation applied to 1D quantum Hamiltonians improves convergence

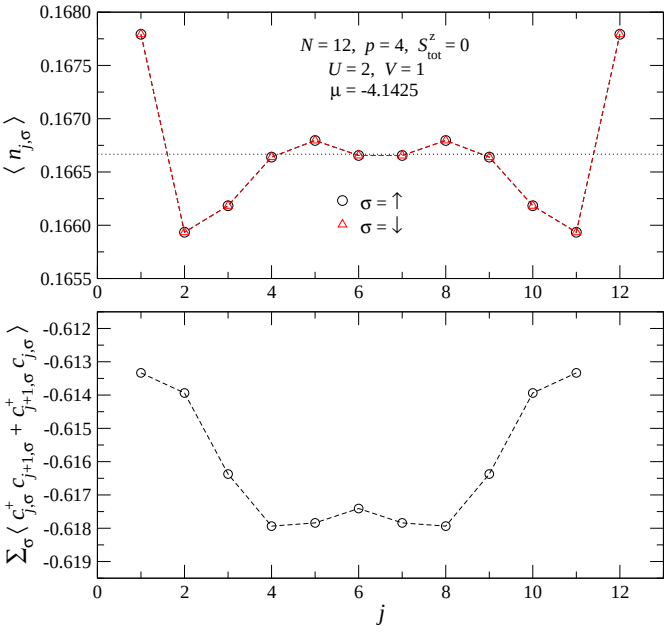


FIG. 12: (Color online) The upper and lower graphs show the occupancy $\langle n_{i,\sigma}\rangle$ and the bond correlation $\sum_\sigma \langle c^\dagger_{j\sigma} c_{j+1\sigma} + c^\dagger_{j+1\sigma} c_{j\sigma}\rangle$ at $f = 1/6$.

of the ground state energy per bond (or per site) $e_0^{(N)}$ toward the thermodynamic limit, compared to the uniform systems with open boundary conditions. Such suppression of the boundary effects is confirmed also for interacting systems, typically for the extended Hubbard model.

We have not determined the 'canonical' form of the sinusoidal deformation in case where there are long-range interactions. It is reported that a small but finite residual boundary effect appears in spin chains which includes the next-nearest-neighbor interaction. [15] Application of the sinusoidal deformation to higher-dimensional quantum systems could be a future problem.

A theoretical puzzle of the sinusoidal deformation remains in coincidence of the ground-state energy calculated with PBC and SSD. The agreement is almost perfect, which strongly suggests a hidden algebraic relation between these two cases.

Acknowledgments

We thank T. Hikihara, A. Feiguin, and K. Okunishi for valuable discussions. This work was supported by ERDF OP R&D, Project "QUTE - Centre of Excellence for Quantum Technologies" (ITMS 26240120009), CE QUTE SAV, APVV-51-003505, VVCE-0058-07, and VEGA-2/0633/09. T. N. acknowledges the support of Grant-in-Aid for Scientific Research (C) No. 22540388.

[1] M.E. Fisher and M.N. Barber, Phys. Rev. Lett. **28**, 1516 (1972).
[2] M.N. Barber, in Phase Transitions and Critical Phenomena Vol. **8**, ed. C. Domb and J.L. Lebowitz (Academic Press, 1983).
[3] T.W. Burkhardt and J.M.J. van Leewen, Real-Space Renormalization, Topics in Current Physics, Vol. **30** (Springer, Berlin, 1982), and references therein.
[4] S.R. White, Phys. Rev. Lett. **69**, 2863 (1992); Phys. Rev. B **48**, 10345 (1993).
[5] I. Peshel, X. Wang, M. Kaulke, and K. Hallberg, Density-Matrix Renormalization, Lecture Notes in Physics, vol. **528** (Springer, Berlin, 1999).
[6] U. Schollwöck. Rev. Mod. Phys. **77**, 259 (2005).
[7] F. Verstraete, D. Porras, and J.I. Cirac, Phys. Rev. Lett. **93**, 227205 (2004).
[8] P. Pippan, S.R. White, and H.G. Evertz, Phys. Rev. B **81**, 081103(R) (2010).
[9] D. Rossini, V. Giovannetti, R. Fazio, arXiv:1102.3562.
[10] D. Rossini, V. Giovannetti, R. Fazio, arXiv:1102.3545.
[11] M. Vekić and S. R. White, Phys. Rev. Lett. **71**, 4283 (1993).
[12] M. Vekić and S. R. White, Phys. Rev. B **53**, 14552 (1996).
[13] A. Gendiar, R. Krcmar, and T. Nishino, Prog. Theor. Phys. **122**, 953 (2009).
[14] The deformation function used in Ref. [13] is $[\sin(j\pi/N)]^2$, although all the deformed Hamiltonians are *denoted with the wrong factor* $[\sin(j\pi/N)]$. This primitive mistake by the authors of Ref. [13] was corrected in the Erratum: A. Gendiar, R. Krcmar, and T. Nishino, Prog. Theor. Phys. **123**, 393 (2010).
[15] T. Hikihara and T. Nishino, to appear in phys. Rev. B; arXiv:1012.0472.
[16] Another generalization is to replace the sinusoidal function by the hyperbolic function: H. Ueda, A. Gendiar, V. Zauner, T. Iharagi, T. Nishino, preprint arXiv/1008.3458.
[17] If the particle number $N/2$ is even, $e_0^{(N)}$ coincides with that obtained for the anti-periodic boundary condition, which is specified by $\alpha = -1$ in Eq. 2. The fact was pointed out in Ref. [16].
[18] The Hamiltonian in Eq. (15) can be mapped to $S = 1/2$ XXZ model by means of Jordan-Wigner transformation. The XXZ model under sine-squared deformation is studied in Ref. [16] under the presence of magnetic field, which plays the role of chemical potential.